HHS Public Access

Author manuscript

Mol Plant Pathol. Author manuscript; available in PMC 2019 May 01.

Published in final edited form as:

Mol Plant Pathol. 2018 May ; 19(5): 1172–1183. doi:10.1111/mpp.12595.

The Agrobacterium VirE2 effector interacts with multiple members of the *Arabidopsis* VIP1 protein family

Luyao Wang[1,2], **Benoît Lacroix**[1,*], **Jianhua Guo**[2], and **Vitaly Citovsky**[1]

[1]Department of Biochemistry and Cell Biology, State University of New York, Stony Brook, NY 11794-5215

[2]Department of Plant Pathology, College of Plant Protection, Nanjing Agricultural University, Key Laboratory of Monitoring and Management of Crop Diseases and Pest Insects, Ministry of Agriculture, Engineering Center of Bioresource Pesticide in Jiangsu Province, Nanjing, Jiangsu Province, 210095, China

Summary

T-DNA transfer from *Agrobacterium* to its host plant genome relies on multiple interactions between plant proteins and bacterial effectors. One of such plant proteins is the *Arabidopsis* VirE2 interacting protein (AtVIP1), a transcription factor that binds *A. tumefaciens* C58 VirE2, potentially acting as an adaptor between VirE2 and several other host factors. It remains unknown, however, whether the same VirE2 protein has evolved to interact with multiple VIP1 homologs in the same host, and whether VirE2 homologs encoded by different bacterial strains/species recognize AtVIP1 or its homologs. Here, we addressed these questions, by systematic analysis - using the yeast-two-hybrid and co-immunoprecipitation approaches - of interactions between VirE2 proteins encoded by four major representatives of known bacterial species/strains with functional T-DNA transfer machineries and eight VIP1 homologs from *Arabidopsis* and tobacco. We also analyzed the determinants of the VirE2 sequence involved in these interactions. These experiments showed that the VirE2 interaction is degenerate: the same VirE2 protein has evolved to interact with multiple VIP1 homologs in the same host, and different and mutually independent VirE2 domains are involved in interactions with different VIP1 homologs. Furthermore, the VIP1 functionality related to the interaction with VirE2 is independent of its function as a transcriptional regulator. These observations suggest that the ability of VirE2 to interact with VIP1 homologs is deeply ingrained into the process of *Agrobacterium* infection. Indeed, mutations that abolished VirE2 interaction with AtVIP1 produced no statistically significant effects on interactions with VIP1 homologs or on the efficiency genetic transformation.

Introduction

During plant genetic transformation mediated by *Agrobacterium* spp., the transferred DNA (T-DNA) in a single-stranded form and several bacterial protein effectors are exported into the host cell cytoplasm. Multiple interactions between different bacterial and host proteins facilitate and control transport of the T-DNA into the cell nucleus and its integration into the

*Corresponding author: benoit.lacroix@stonybrook.edu.

host genome (Gelvin, 2003, Lacroix & Citovsky, 2013b). Some host factors interacting with *Agrobacterium* effectors represent housekeeping cellular pathways and are diverted from their native functions to facilitate T-DNA transfer whereas others represent host responses aimed at controlling or preventing *Agrobacterium* infection. Within the host cell, two of the bacterial effectors are thought to associate with the transported T-DNA molecule: VirD2 and VirE2. VirD2 is covalently attached to the 5′ end of the T-DNA strand (Young & Nester, 1988, Ward & Barnes, 1988). VirE2 is a single-stranded (ss) DNA binding protein (Citovsky *et al.*, 1989, Christie *et al.*, 1988, Sen *et al.*, 1989) that packages ssDNA in a helical nucleoprotein complex (Citovsky *et al.*, 1997, Abu-Arish *et al.*, 2004), suggesting that VirE2 plays a role in protecting the T-DNA from degradation and mediating its interactions with host factors.

One of the plant proteins that interact with VirE2 is VIP1 (VirE2 interacting protein 1), a transcription factor of the bZIP family (Tzfira *et al.*, 2001), involved in stress response (Djamei *et al.*, 2007, Pitzschke *et al.*, 2009) and osmosensory and touch responses (Tsugama *et al.*, 2014, Tsugama *et al.*, 2016). VIP1 has been suggested to act as a molecular adapter between VirE2 and several host cell factors, such as importins alpha of the nuclear import pathway (Tzfira et al., 2001, Tzfira *et al.*, 2002, Citovsky *et al.*, 2004), plant and bacterial F-box proteins, such as VirF and VBF, of the proteasomal degradation pathway (Tzfira *et al.*, 2004, Zaltsman *et al.*, 2010, Zaltsman *et al.*, 2013), and nucleosomal histones (Loyter *et al.*, 2005, Lacroix *et al.*, 2008). However, a recent study challenged the role(s) of VIP1 in the *Agrobacterium*-plant cell interaction; using a root assay in *Arabidopsis thaliana*, it was reported that *Agrobacterium*-mediated transformation efficiency was not affected in an *Arabidopsis* line with an insertional mutation in the *VIP1* gene (Shi *et al.*, 2014). Potentially, this could be due to overlapping activities of numerous VIP1 homologs encoded by the *Arabidopsis* genome that are redundant in their subcellular localization and transcriptional activation function (Tsugama et al., 2014). Furthermore, although VirE2 is important for T-DNA transfer, it is not absolutely necessary, and a *vir*E2 mutant of *A. tumefaciens* retains a low level of virulence (Stachel *et al.*, 1985, Horsch *et al.*, 1986). This is consistent with the diversity of the potential pathways involved in *Agrobacterium*-mediated genetic transformation of plants. Here we explore this diversity by investigating the interactions between VirE2 from different bacterial strains and several members of the VIP1 family in *Arabidopsis* and tobacco and the determinants of the VirE2 sequence involved in these interactions.

Results

Homologs of AtVIP1 in *A. thaliana* and other plant species

VIP1 belongs to the large family of bZIP (basic region/leucine zipper) domain transcription factors, present in all eukaryotes whose genomes have been sequenced so far; the bZIP protein family of *Arabidopsis* comprises 75 members—four times more than yeast, worm or human—involved in such diverse processes as plant development, light signaling, and biotic and abiotic stress responses (Jakoby *et al.*, 2002). Based on basic region sequence similarity and on the presence of conserved motifs, *Arabidopsis* bZIP proteins have been clustered in 10 groups (Jakoby et al., 2002). AtVIP1 belongs to group I; within this group, phylogenetic

analysis defined several subgroups, with AtVIP1 and six other bZIP proteins belonging to subgroup 1 (Tsugama et al., 2014). Homologs of AtVIP1 are encoded by genomes of many other plant species. Fig. 1 shows a phylogenetic tree of 38 of the closest homologs of AtVIP1 in different species from the main taxa of higher plants (summarized in Table S1) suggests that most plant species in the angiosperm group encode proteins closely related to AtVIP1, forming a clade distinct from the rest of the *Arabidopsis* bZIP proteins of the subgroup I-1. Generally, the phylogeny of the VIP1 homologs reflects the phylogeny of the species, e.g., VIP1-like proteins from monocotyledonous plants are grouped in a single clade, distinct from the VIP1-like sequences from dicotyledonous plants. Thus, bZIP proteins from other angiosperm species that are closely related to AtVIP1 likely represent AtVIP1 orthologs. We selected all proteins from the *Arabidopsis* subgroup I-1, i.e., VIP1, bZIP18, bZIP52, bZIP69, posF21, bZIP29, and bZIP30, as well as the *Nicotiana tabacum* VIP1 ortholog NtRSG (Fig. 1) as an example of a non-*Arabidopsis* VIP1-like protein, to examine their potential interactions with VirE2.

Interactions between VirE2 from different bacterial strains and AtVIP1 and its homologs

Initially, we examined potential interactions between VirE2 from *Agrobacterium* C58 and VIP1 homologs in a yeast-two-hybrid system, in which cell growth on a histidine-deficient medium indicates interaction. Fig. 2A shows that VirE2 interacted with five out of six *Arabidopsis* VIP1 homologs tested, i.e., bZIP52, bZIP69, posF21, bZIP29, and bZIP30 as well as with VIP1 and NtRSG, but not with bZIP18. This interaction ability of VirE2 was specific because it was not observed with an unrelated control protein, the cell-to-cell movement protein (MP) of the *Tobacco mosaic virus* (TMV) (Citovsky *et al.*, 1990, Wolf *et al.*, 1989) (Fig. 2A). To demonstrate further the selectivity of these interactions, we utilized 3-amino-1,2,4-triazole (3-AT), a competitive inhibitor of the *HIS3* gene product, which selects for stronger interactions that produce enough histidine to sustain the inhibition and allow cell survival. Indeed, under these conditions, we still observed the identified interactions of VirE2 with VIP1 homologs (Fig. 2A). Conversely, the negative control TMV MP promoted only weak cell growth, which was completely suppressed by 3-AT (Fig. S1), indicating lack of TMV MP interaction with any of the tested VIP1 homologs. Under non-selective conditions, i.e., in the presence of histidine, all combinations of the tested proteins resulted in the efficient cell growth, indicating that none of the constructs interfered with cell viability (Fig. 2A, Fig. S1). Notably, histidine prototrophy alone may also detect weak two-hybrid interactions, which may or may not affect the functional relevance of these interactions.

The yeast-two-hybrid results were then validated by an independent approach, in which individual VIP1 homologs tagged with GFP were coexpressed in *N. benthamiana* leaves with C58 VirE2 tagged with the Myc epitope and immunoprecipitated with anti-GFP antibody followed by western blot analysis. Fig. 2B shows that the resulting immunoprecipitates contained both VIP1 homologs detected by anti-GFP and VirE2 detected by anti-Myc; note that both fusion proteins are expected to have relative electrophoretic mobility in the range of 58–80 kDa. These results confirm the data obtained in the two-hybrid system and indicate that the latter can serve as a reliable assay for VirE2-VIP1 interactions. Collectively, the data in Fig. 2 support the notion that C58 VirE2 can

interact with numerous VIP1 homologs, i.e., bZIP52, bZIP69, posF21, bZIP29, and bZIP30, VIP1, and NtRSG, in plant cells.

Next, we investigated whether VirE2 proteins encoded by other *Agrobacterium* and *Rhizobium* species/strains can interact with AtVIP1 and its homologs. Specifically, we selected *vir*E2 sequences from the octopine-type *A. tumefaciens* A6, *A. vitis* S4, and *R. etli* CFN42; along with the nopaline-type *A. tumefaciens* C58, these bacterial strains represent the major known examples of plant-infecting bacteria containing a functional virulence region that can transfer T-DNA to plants. Fig. 3 shows that each of these VirE2 proteins has the ability to bind VIP1 and/or its homologs, but with different binding specificity. The yeast two-hybrid analysis under stringent selection conditions in the presence of 0.1–5.0 mM 3-AT demonstrated that A6 VirE2 had a relatively narrow specificity, detectibly interacting with bZIP18, VIP1, and NtRSG. In contrast, S4 VirE2 had broad specificity, interacting with all tested VIP1 homologs, with the most prominent interactions observed with bZIP18, bZIP52, VIP1, and NtRSG; similarly, CFN42 VirE2 also interacted with all VIP1 homologs, except bZIP30, and most prominently with bZIP18 and VIP1 (Fig. 3). Interestingly, bZIP18 that interacted well with A6 VirE2, S4 VirE2, and CFN42 VirE2, was the only VIP1 homolog that was not recognized by C58 VirE2. Without selection, all combinations of the tested proteins resulted in comparable cell growth (Fig. 3). Thus, the ability to bind to VIP1 and its homologs appears to be conserved for VirE2 proteins from the four major representatives of known bacterial species/strains with functional T-DNA transfer machineries, suggesting that it may represent a key aspect of their activity.

Transcription factor activity and subcellular localization of AtVIP1 homologs

VIP1 is a transcription factor that regulates numerous genes involved mostly in stress and defense responses (Pitzschke et al., 2009) and in osmosensing (Tsugama *et al.*, 2012). Although VIP1 homologs have been shown to possess similar transcriptional activation abilities in the osmosensory response (Tsugama et al., 2014), their potentially redundant activity in activating defense signaling regulatory sequences has not been examined. These sequences include a short DNA hexamer motif that acts as the VIP1 response element (*VRE*) (Pitzschke et al., 2009). To monitor VIP1 activation of *VRE* we have developed a reporter system, in which direct tandem repeat of the *VRE* sequence is fused to the CaMV 35S minimal promoter that drives expression of GFP (Lacroix & Citovsky, 2013a). Here, we took advantage of this system to measure the ability of VIP1 homologs to activate the *VRE*-controlled reporter. Fig. 4A shows that bZIP18, bZIP52, bZIP69, and NtRSG, as well as the positive control VIP1, induced *VRE*, resulting in GFP expression, whereas posF21, bZIP29, and bZIP30 lacked this activity. That the endogenous VIP1 did not detectably activate GFP expression is consistent with the known naturally low levels of this protein in plant cells (Tzfira et al., 2001, Tzfira et al., 2002). The GFP signal induced by VIP1 homologs was then quantified relative to the induction by VIP1. Fig. 4B shows that bZIP18, bZIP52, bZIP69, and NtRSG activated the *VRE*-controlled reporter with efficiencies ranging from 20 to 50% of the activity observed with VIP1.

Unlike their effects on induction of *VRE*, all VIP1 homologs displayed similar subcellular localization. Fig. 5 shows that GFP-tagged bZIP18, bZIP52, bZIP69, posF21, bZIP29,

bZIP30, and NtRSG partitioned between the cell cytoplasm and the nucleus. The same nucleocytoplasmic distribution pattern was observed for the full-length VIP1 protein here (Fig. 5) and in previous studies (Djamei et al., 2007, Tsugama et al., 2012). Thus, the similar subcellular localization patterns of these VIP1 homologs are consistent with their general functionality as transcription factors, yet the specificity of their promoter response elements differs between different groups of the members of the family. Interestingly, these differences between the VIP1 homologs in their specificity of promoter recognition do not correlate with the differences in their ability to bind VirE2. Thus, the determinants that define the natural function of the VIP1 homologs in regulation of gene expression likely differ from the determinants that define their interaction with VirE2 and, possible involvement in *Agrobacterium* infection.

C58 VirE2 sequence determinants involved in binding to AtVIP1 and AtVIP1 homologs

Interaction between C58 VirE2 and AtVIP1 has been proposed to rely on two small central domains in the protein, i.e., amino acid residues 278–293 and 323–338, based on *in vitro* peptide interaction assays (Maes *et al.*, 2014). To explore the role of these two domains further, we generated a series of deletion mutations (Fig. 6A), and tested them for the ability to interact with AtVIP1 and its homologs in the yeast-two-hybrid system, followed by validation of the resulting data by coimmunoprecipitation. Initially, the mutants were tested for interaction with VIP1, and Fig. 6A shows that two mutants that did not contain the central domains, i.e., mutants 1–250 and 350–556, showed only residual levels of binding; these mutants were not toxic to yeast because, without selection, they allowed cell growth indistinguishable from that observed with other tested mutants. In contrast, the presence of both or either one of the central domains was sufficient for apparent wild-type levels of interactions, virtually irrespective of the identity of other VirE2 sequences present in each mutant (Fig. 6A). Amino acid sequence alignment of the two central domains between C58 VirE2, A6 VirE2, S4 VirE2, and CFN42 VirE2 showed an overall conservation as well as the presence of a conserved FAGD/E motif in each of the domains (Fig. 6B). Based on this sequence analysis, we selected 12 amino acid residues, i.e., G280, D281, K286, F288, E290, W323, E324, R325, R331, F335, G337, E338, conserved between the two central domains of all four bacterial strains/species and located within and outside the FAGD/E motifs; we also aimed to include charged amino acids that might be involved in protein-protein interactions. We used alanine scanning mutagenesis to substitute alanine for these 12 residues and produced a series of single, double, triple, and quadruple combinations of such substitutions; the resulting mutants were tested for interaction with VIP1 in the yeast two-hybrid system (Fig. S2).

Most single, double, and triple mutants retained some ability to interact with VIP1, although with different efficiency. For example, D281A, E324A, and R331A, and most double or triple mutants that contained one of these mutations showed reduced binding (Fig. S2). Remarkably, however, one quadruple mutant of C58 VirE2, i.e., D281A/E324A/R331A/E338A (Fig. 6B, arrows), which was designated C58 VirE2 4M, the interaction with VIP1 was virtually abolished (Fig. S2). We then tested C58 VirE2 4M for its ability to interact with VIP1 homologs. Fig 6C shows that C58 VirE2 4M still interacted with bZIP52, bZIP69, posF21, bZIP29, and bZIP30, albeit relatively weakly compared to their

interactions with the wild-type C58 VirE2 whereas the interaction with NtRSG did not appear to be affected (compare Fig. 6C to Fig. 2A). A similar pattern of interactions was observed with the deletion mutant C58 VirE2 350–556 (Fig. 6D), suggesting this C-terminal segment of the protein, that lacks the two central domains required for binding to VIP1, likely contains sequences that allow interaction with NtRSG and the five *Arabidopsis* VIP1 homologs, although there is no apparent sequence homology between the 350–556 segment of C58 VirE2 and any of the two central domains required for interaction with AtVIP1. As expected VIP1, bZIP18, and TMV MP showed no interactions with C58 VirE2 4M or C58 VirE2 350–556, and growth under non-selective conditions showed no effects of any of the tested protein combinations on cell viability (Fig. 6C, D). The pattern of C58 VirE2 4M interactions with VIP1 and its homologs was confirmed by coimmunoprecipitation. Fig. 6E shows that Myc-tagged C58 VirE2 44M coexpressed in *N. benthamiana* leaves with GFP-tagged VIP1or its different homologs and immunoprecipitated with anti-GFP antibody coprecipitated with bZIP52, bZIP69, posF21, bZIP29, and bZIP30, as detected by western blotting with anti-Myc antibody (lanes 3–8), whereas no such coimmunoprecipitation was observed for C58 VirE2 4M-Myc coexpressed with GFP-VIP1, GFP-bZIP18, or GFP-TMV MP (lanes 1, 2, 7). Taken together, these data support the idea of different C58 VirE2 sequence determinants involved in interactions with VIP1 and its homologs.

Finally, we examined the ability of C58 VirE2 4M to transform genetically *Nicotiana* and *Arabidopsis* tissues. To this end we used the oncogenic *Agrobacterium vir*E2 insertional mutant strain mx358 which does not express functional VirE2 (Stachel et al., 1985) and which was complemented with a construct expressing, from the native *vir*E promoter, either the wild-type C58 VirE2 or C58 VirE2 4M. In *Nicotiana*, transient genetic transformation was monitored in leaf tissues by expression of a GFP reporter transgene whereas stable transformation was monitored by formation of tumors on inoculated leaf disks. In *Arabidopsis*, transient genetic transformation was monitored by expression of a *gus* gene for the β-glucuronidase (GUS) reporter in root segments and stable transformation was monitored by a root tumor assay (Gelvin, 2006). Fig. 7A shows that both C58 VirE2 and C58 VirE2 4M allowed transient expression of the GFP transgene in *Nicotiana* leaves, with no such expression observed with a control construct, lacking the *vir*E2 gene. Both C58 VirE2 and C58 VirE2 4M also complemented the bacterial tumorigenicity whereas no tumors were observed with the control plasmid, i.e., in the absence of VirE2 (Fig. 7B). Quantification of these data by measuring the GFP signal and weighing the tumors suggested that C58 VirE2 4M exhibited a slightly lower transformation efficiency (Fig. 7C, D), yet these differences were not statistically significant, with P values higher than 0.05. The values obtained with the control plasmid were low, and they represented the background readings of each quantification method. Similarly, we did not detect statistically significant differences between C58 VirE2 and C58 VirE2 4M in their ability to complement the bacterial capacity for transient and stable transformation of *Arabidopsis* roots (Fig. 7E–G). These data are consistent with our observations that the 4M mutation, although blocking the VirE2 interaction with VIP1, had no effect on its interactions with *Nicotiana* NtRSG or with five *Arabidopsis* VIP1 homologs (see Fig. 6C).

Discussion

The proposed involvement of the *Arabidopsis* bZIP protein VIP1 in *Agrobacterium* infection is consistent with its known roles in different types of biotic and abiotic stress (Djamei et al., 2007, Pitzschke et al., 2009, Tsugama et al., 2014, Tsugama et al., 2016). Yet, a recent study suggested that a loss-of-function mutant of VIP1 is still susceptible to infection (Shi et al., 2014). One possible explanation is the redundant function of one or more of the 75 members of the large bZIP family, especially those 6 proteins that belong to the VIP1 subgroup. Thus, it was important to examine possible interactions of VirE2 with these VIP1 homologs. Indeed, our data demonstrate that, in addition to VIP1, VirE2 from a nopaline-type pTi58 plasmid interacts with five *Arabidopsis* VIP1 homologs as well as with a homolog from tobacco. Importantly, the ability to interact with the members of the VIP1 family is conserved between VirE2 proteins from such diverse bacteria as nopaline and octopine-type *A. tumefaciens* C58 and A6, *A. vitis* S4, and *R. etli* CFN42, all of which encode a functional protein machinery for T-DNA transfer to plants. This conserved capability of recognition of VIP1-like proteins on the pathogen side is complemented by the conserved nature of the VIP1-like proteins on the host plant side, at least among the angiosperms.

That the T-DNA transfer capacity parallels preservation of the VirE2-VIP1 interaction across different bacterium-host strains/species, and the observed “degeneracy” of the VirE2-VIP1 interaction, i.e., that the same VirE2 protein has evolved to interact with multiple VIP1 homologs in the same host, suggest a role for this interaction in the genetic transformation mechanism. On the other hand, specific VirE2 proteins showed different, yet overlapping, specificities toward individual VIP1 homologs, potentially affecting the host range of the different bacterial species. This subset of VIP1 homologs share somewhat redundant biological functions in uninfected cells (Van Leene *et al.*, 2016, Tsugama et al., 2014, Tsugama et al., 2016), which suggests that this redundancy also could apply to their interactions with VirE2 during the infection process. Whereas, in nature, the host range of *Agrobacterium* is essentially limited to dicotyledonous plants, under laboratory conditions many more eukaryotic species can be transformed by *Agrobacterium*, from monocotyledonous plants, to yeast and other fungi, to mammalian cultured cells (Lacroix *et al.*, 2006). As at least some of these species do not encode a close homolog of VIP1, most likely they are transformed via alternative (and potentially less efficient) pathways, which may in part explain the low efficiency of genetic transformation of mammalian cells by the wild-type T-DNA transfer machinery (Kunik *et al.*, 2001) or of plant cells by a VirE2-deficient T-DNA transfer machinery (Horsch et al., 1986, Stachel & Nester, 1986).

The degeneracy of the VirE2-VIP1 interaction also manifested in different and mutually independent VirE2 determinants involved in interactions with different VIP1 homologs, such that a VirE2 mutant that does not bind VIP1 still interacts with other members of this family. Specifically, for interaction of C58 VirE2 with VIP1, one of the two conserved central domains of VirE2 was necessary and sufficient, but they did not appear to be involved in binding to VIP1 homologs. Furthermore, a truncated mutant corresponding to the C-terminal half of the protein and lacking the two central domains retained the ability to interact with VIP1 homologs, indicating that this part of VirE2 contains another domain responsible for these interactions, although we were unable to detect conserved motifs in this sequence.

The nucleocytoplasmic localization of the *Arabidopsis* homologs of VIP1 was similar to that of VIP1 itself, consistent with their presumably similar biological roles of transcriptional regulators. Yet, they differed from VIP1 in their ability to recognize the VIP1 response element *VRE* and induce reporter expression, with no clear correlation with their common ability to interact with VirE2. This suggests that different domains of the VIP1 homologs are involved in these two different activities, and that the VIP1 functionality related to the interaction with VirE2 is independent of its function as a transcriptional regulator.

Collectively, the almost ubiquitous ability to interact with VirE2 among VIP1 homologs, involvement of different VirE2 domains in interactions with different VIP1 homologs, and relative independence of these interactions on the specificity of VIP1 homologs as transcriptional activators suggest that this functionality is deeply insinuated into the process of *Agrobacterium* infection. Indeed, mutations that completely abolished the C58 VirE2 ability to interact with VIP1 produced no statistically significant effect on interactions with VIP1 homologs, *Arabidopsis* or *Nicotiana*, or on the efficiency of the transient and stable genetic transformation of these plants. This preservation of the VirE2-VIP1 interaction across different bacterial species/strains and different VIP1 homologs makes the alternative explanation that this interaction is not involved in transformation unlikely, yet it cannot be ruled out. In addition, infection assays performed under laboratory conditions could influence the efficiency and the lack of requirements for the VirE2-VIP1 interaction. Thus, it would be particularly interesting to understand whether interactions of VirE2 with VIP1 homologs might affect the host range of the different *Agrobacterium* strains and/or influence the efficiency of transformation of a given host plant species in nature.

Experimental Procedures

Bacterial strains and cultures

Wild-type *Agrobacterium tumefaciens* strains A6 (octopine-type) and C58 (nopaline-type), *Agrobacterium vitis* S4 (a kind gift from Dr. Thomas J. Burr, Cornell University, Ithaca, NY) and *Rhizobium etli* CFN42 (kindly provided by Dr. Russell Carlson, University of Georgia, Athens, GA) were used for plasmid extraction and cloning of the *vir*E2 coding sequences. *A. tumefaciens* strain EHA105, a disarmed C58 derivative, harboring the pMP90 helper plasmid, and the mx358 *vir*E2 insertional mutant in the A348 background (Stachel et al., 1985) were used for *N. benthamiana* leaf infiltration and tobacco leaf discs or *Arabidopsis* root transformation experiments. All *A. tumefaciens* strains were grown in LB medium at 28°C; *R. etli* was grown in TY medium (5 $g.L^{-1}$ tryptone, 3 $g.L^{-1}$ yeast extract, and 10 mM $CaCl_2$) at 28°C. The *E. coli* strain DH5α was used for molecular cloning and grown in LB medium at 37°C.

Plants

Nicotiana benthamiana plants were grown in soil. *Arabidopsis thaliana* (ecotype Col-0) plants were grown on MS based medium (0.5 $g.L^{-1}$ MES, 10 $g.L^{-1}$ sucrose, 8 $g.L^{-1}$ agar, pH 5.8) after seed surface sterilization. *Nicotiana tabacum* var. Turk plants were micro-propagated *in vitro* on high-sucrose MS medium (0.5 $g.L^{-1}$ MES, 30 $g.L^{-1}$ sucrose, 8 $g.L^{-1}$

agar, pH 5.8). All plants were grown in environment-controlled growth chambers under long-day conditions (16 h light/8 h dark cycle at 140 μE $sec^{-1}m^{-2}$ light intensity) at 22°C.

Protein sequence analyses

Homologs of the AtVIP1 sequences in plant species were identified in sequence databases using the blastp program (PubMed); for each species, the sequence with the highest score was selected. VIP1 homolog phylogenetic tree was generated using MEGA version 6 (Tamura *et al.*, 2013). Protein sequence alignments were performed with the T-Coffee (Notredame *et al.*, 2000) and Boxshade programs.

Plasmid construction and mutagenesis

Plasmids and cloning strategies are described in Table S2, and primer sequences used in these cloning procedures are summarized in Table S3. For Gal4-AD fusions, the coding sequences of VIP1, VIP1 homologs, and TMV MP were PCR-amplified, using total *A. thaliana* Col-0 cDNA as substrate, and cloned into the indicated sites of pGAD424 (LEU2+, Clontech; Mountain View, CA). For LexA fusions, the coding sequences of *vir*E2 and its mutant variants were PCR-amplified, using purified Ti-plasmids from the corresponding *Agrobacterium* or *Rhizobium* strains, and cloned into the indicated sites of pSTT91 (TRP1+) (Sutton *et al.*, 2001). To generate point mutations in C58 *virE2*, overlapping PCR reactions with the indicated primers were carried out to introduce codon substitutions. Two DNA segments were amplified by PCR: from the translation initiation codon at the 5′-end to the target codon position and from the target codon position to the 3′ end of the coding sequence. For example, to introduce the D281A mutation, PCR reactions were performed with the primer pairs 8F-17R and 17F-8R (Table S3). The two PCR products then were used as template to generate the full length mutated *vir*E2 sequence by overlapping PCR with the primer pair 8F-8R, followed by insertion of the resulting PCR product, that encodes the full-length C58 VirE2 D281A mutant, into the BamHI/PstI site of plasmid pSTT91, resulting in pSTT91-C58*vir*E2-D281A (Table S2). For coimmunoprecipitation, C58 *vir*E2 and C58 *vir*E2 4M coding sequences were PCR-amplified and inserted into the HindIII-KpnI sites of pSAT5-Myc-N1 (Magori & Citovsky, 2011). For expression in plants, the coding sequences of VIP1 and its homologs were inserted into the indicated sites of pSAT5A-MCS (Tzfira *et al.*, 2005) to be used in transcriptional activation experiments, or pSAT5-GFP-C1 (Tzfira et al., 2005) to be used in subcellular localization experiments. The resulting expression cassettes were excised with ICeuI and transferred into the same site of the binary pPZP-RCS2 vector (Tzfira et al., 2005). The binary plasmid pCB302T-VRE1-GFP for VIP1-induced expression of the GFP reporter was described previously (Lacroix & Citovsky, 2013a). For expression in *Agrobacterium* cells, the full *vir*E promoter was amplified from pTiA6 with the primer pair F29/R29 and introduced into the BspHI(NcoI)/EcoRI sites of pEp (Lacroix & Citovsky, 2011), producing pEpA6. Then, the coding sequences of C58 VirE2 and C58 *vir*E2 4M were amplified from pSTT91-C58*vir*E2 or pSTT-C58*vir*E2-4M, respectively, with the primer pair F30/R30, and cloned into the NheI/KpnI sites of pEpA6. For monitoring transient T-DNA expression in *Arabidopsis* roots and tobacco leaf discs, we used binary plasmids pBISN1 with an expression cassette for a *gus* reporter gene with a plant intron sequence (*gus*-int) (Narasimhulu *et al.*, 1996), and pCB302T-GFP carrying an expression cassette for EGFP (Lacroix & Citovsky, 2016), respectively.

Yeast-two-hybrid protein interaction assay

The assay was performed using the yeast strain L40 (Hollenberg *et al.*, 1995), cotransformed with pSTT91- and pGAD424-derived construct expressing the tested protein pairs. Five to ten colonies obtained on plates with synthetic defined premixed yeast growth medium (TaKaRa Clontech) lacking leucine and tryptophan (SD-Leu-Trp) were resuspended in water and plated at indicated dilutions on SD-Leu-Trp and on SD the same medium lacking leucine, tryptophan and histidine (SD-Leu-Trp-His) supplemented with the indicated concentrations of 3-amino-1′, 2′, 4′ triazole (3-AT). Cell growth was recorded after incubation for 2–3 days at 28°C.

Coimmunoprecipitation

Coimmunoprecipitation experiments were performed as described (Magori & Citovsky, 2011), with some modifications. Briefly, the tagged proteins were transiently expressed in *N. benthamiana* leaves after agroinfiltration as described (Lacroix & Citovsky, 2011), and, after 72 h, infiltrated leaves were harvested and ground into fine powder in liquid nitrogen. Total proteins were extracted from the ground tissues in IP buffer [50 mM Tris-HCl pH 7.5, 150 mM NaCl, 0.1% NP-40, 1 mM EDTA, 3 mM dithiothreitol (DTT), 1× plant protease inhibitor cocktail (Amresco)]. Protein extracts were incubated with anti-GFP antibody (Clontech, dilution 1:250) for 3 hours at 4°C, followed by incubation with Protein G-Sepharose 4B (Invitrogen) for an additional 3 hours at 4°C to capture and precipitate the immune complexes. After three washes with washing buffer (50 mM Tris-HCl pH 7.5, 150 mM NaCl, 0.1% NP-40, and 1 mM EDTA), immunoprecipitates were eluted in SDS sample buffer and subjected to western blot analysis. GFP- and My-tagged proteins were detected by immunoblotting with anti-GFP antibody (Clontech, dilution 1:2000) and anti-cMyc antibody (Genscript, dilution 1:2000), respectively, followed by a secondary antibody conjugated to horseradish peroxidase (ThermoFisher Scientific, dilution 1:2000).

Agroinfiltration and confocal microscopy

For agroinfiltration, the *Agrobacterium* strain EHA105 (Lacroix & Citovsky, 2013a) harboring the appropriate binary constructs was grown overnight at 25°C, diluted to OD_{600}=0.3, and infiltrated into intact *N. benthamiana* leaves as described (Lacroix & Citovsky, 2011). The leaves were harvested 3 days after agroinfiltration and analyzed under a Zeiss (Oberkochen, Germany) LSM 5 Pascal confocal laser scanning microscope. Three plants were used per each experimental condition, and all experiments were repeated at least three times.

Transient and stable transformation assays

Transient expression assays in *N. benthamiana* were performed exactly as described (Lacroix & Citovsky, 2011). Tumor assays in *N. tabacum* leaf discs were performed following the classical leaf disc transformation procedure (Horsch *et al.*, 1985). An overnight culture of *A. tumefaciens* in LB supplemented with antibiotics was diluted in LB without antibiotics, grown for 3–4 h and adjusted to a cell density of OD_{600nm}= 0.5. Leaf discs (9 mm) from fully expanded leaves of 4-week old tobacco plants were immersed for 10 min in the *Agrobacterium* suspension culture, placed on MS medium and incubated for 48 h

in a growth chamber. Leaf discs were then rinsed in sterile water with 100 mg.L^{-1} timentin, placed on MST medium and incubated for three weeks, after which the weight of tumors was recorded.

Transient and stable *Arabidopsis* root transformation assays were performed as described (Gelvin, 2006). Root bundles of 14-day-old *Arabidopsis* seedlings aseptically grown on MS medium were collected, cut in 0.5 cm-long segments and transferred onto MS medium. Root segment bundles were covered with approximately 0.5 mL of bacterial suspension (OD_{600nm}=0.1). After a 10-min incubation, the excess of bacterial suspension was removed by pipetting, and the plates were placed in a growth chamber (22°C, long day conditions) for 2 days. The root segments were then rinsed 3 times in sterile water with 100 mg.L^{-1} timentin. For GUS histochemical staining, root segments were incubated on MST medium (MS supplemented with 300 mg.L^{-1} timentin) for 3 days, transferred into a GUS staining solution (50 mM phosphate buffer pH 7.0, 15 mM EDTA, 0.1 % Tween 20, 10 g.L^{-1} X-Gluc), and incubated overnight at 37°C. For tumorigenesis assays, the roots were transferred onto MST plates and incubated for 3 weeks before observation.

Supplementary Material

Refer to Web version on PubMed Central for supplementary material.

Acknowledgments

We would like to thank Dr. Thomas J. Burr (Cornell University, Ithaca, NY) and Dr. Russell Carlson (University of Georgia, Athens, GA) for the kind gift of *Agrobacterium vitis* S4 and *Rhizobium etli* CFN42, respectively, as well as Dr. Stanton B. Gelvin (Purdue University, IN) for the pBISN1 plasmid. The work in the V.C. laboratory is supported by grants from NIH (GM50224), NSF (MCB 1118491), USDA/NIFA (2013-02918), and BARD (IS-4605-13C) to V.C. L.W. is supported by Jiangsu academy of agricultural sciences independent innovation project (CX(15)1004), the National Natural Science Foundation of China (31471812; 31672075) and China Scholarship Council (No. 201506850021).

References

Abu-Arish A, Frenkiel-Krispin D, Fricke T, Tzfira T, Citovsky V, Wolf SG, et al. Three-dimensional reconstruction of *Agrobacterium* VirE2 protein with single-stranded DNA. J Biol Chem. 2004; 279:25359–25363. [PubMed: 15054095]

Christie PJ, Ward JE, Winans SC, Nester EW. The *Agrobacterium tumefaciens virE2* gene product is a single-stranded-DNA-binding protein that associates with T-DNA. J Bacteriol. 1988; 170:2659–2667. [PubMed: 2836366]

Citovsky V, Guralnick B, Simon MN, Wall JS. The molecular structure of *Agrobacterium* VirE2-single stranded DNA complexes involved in nuclear import. J Mol Biol. 1997; 271:718–727. [PubMed: 9299322]

Citovsky V, Kapelnikov A, Oliel S, Zakai N, Rojas MR, Gilbertson RL, et al. Protein interactions involved in nuclear import of the *Agrobacterium* VirE2 protein *in vivo* and *in vitro*. J Biol Chem. 2004; 279:29528–29533. [PubMed: 15123622]

Citovsky V, Knorr D, Schuster G, Zambryski PC. The P30 movement protein of tobacco mosaic virus is a single-strand nucleic acid binding protein. Cell. 1990; 60:637–647. [PubMed: 2302736]

Citovsky V, Wong ML, Zambryski PC. Cooperative interaction of *Agrobacterium* VirE2 protein with single stranded DNA: implications for the T-DNA transfer process. Proc Natl Acad Sci USA. 1989; 86:1193–1197. [PubMed: 2919168]

Djamei A, Pitzschke A, Nakagami H, Rajh I, Hirt H. Trojan horse strategy in *Agrobacterium* transformation: abusing MAPK defense signaling. Science. 2007; 318:453–456. [PubMed: 17947581]

Felsenstein J. Confidence limits on phylogenies: an approach using the bootstrap. Evolution; international journal of organic evolution. 1985; 39:783–791. [PubMed: 28561359]

Gelvin SB. *Agrobacterium*-mediated plant transformation: the biology behind the "gene-jockeying" tool. Microbiol Mol Biol Rev. 2003; 67:16–37. [PubMed: 12626681]

Gelvin SB. *Agrobacterium* transformation of *Arabidopsis thaliana* roots: a quantitative assay. Methods Mol Biol. 2006; 343:105–114. [PubMed: 16988337]

Hollenberg SM, Sternglanz R, Cheng PF, Weintraub H. Identification of a new family of tissue-specific basic helix-loop-helix proteins with a two-hybrid system. Mol Cell Biol. 1995; 15:3813–3822. [PubMed: 7791788]

Horsch RB, Fry JE, Hoffman NL, Eichholtz DA, Rogers SG, Fraley RT. A simple and general method for transferring genes into plants. Science. 1985; 227:1229–1231. [PubMed: 17757866]

Horsch RB, Klee HJ, Stachel S, Winans SC, Nester EW, Rogers SG, et al. Analysis of Agrobacterium tumefaciens virulence mutants in leaf discs. Proceedings of the National Academy of Sciences of the United States of America. 1986; 83:2571–2575. [PubMed: 3458219]

Jakoby M, Weisshaar B, Dröge-Laser W, Vicente-Carbajosa J, Tiedemann J, Kroj T, et al. bZIP transcription factors in *Arabidopsis*. Trends Plant Sci. 2002; 7:106–111. [PubMed: 11906833]

Kunik T, Tzfira T, Kapulnik Y, Gafni Y, Dingwall C, Citovsky V. Genetic transformation of HeLa cells by *Agrobacterium*. Proc Natl Acad Sci USA. 2001; 98:1871–1876. [PubMed: 11172043]

Lacroix B, Citovsky V. Extracellular VirB5 enhances T-DNA transfer from *Agrobacterium* to the host plant. PLOS ONE. 2011; 6:e25578. [PubMed: 22028781]

Lacroix B, Citovsky V. Characterization of VIP1 activity as a transcriptional regulator *in vitro* and *in planta*. Sci Rep. 2013a; 3:2440. [PubMed: 23942522]

Lacroix B, Citovsky V. The roles of bacterial and host plant factors in *Agrobacterium*-mediated genetic transformation. Int J Dev Biol. 2013b; 57:467–481. [PubMed: 24166430]

Lacroix B, Citovsky V. A functional bacterium-to-plant DNA transfer machinery of *Rhizobium etli*. PLOS Pathog. 2016; 12:e1005502. [PubMed: 26968003]

Lacroix B, Loyter A, Citovsky V. Association of the *Agrobacterium* T-DNA-protein complex with plant nucleosomes. Proc Natl Acad Sci USA. 2008; 105:15429–15434. [PubMed: 18832163]

Lacroix B, Tzfira T, Vainstein A, Citovsky V. A case of promiscuity: *Agrobacterium*'s endless hunt for new partners. Trends Genet. 2006; 22:29–37. [PubMed: 16289425]

Loyter A, Rosenbluh J, Zakai N, Li J, Kozlovsky SV, Tzfira T, et al. The plant VirE2 interacting protein 1. A molecular link between the *Agrobacterium* T-complex and the host cell chromatin? Plant Physiol. 2005; 138:1318–1321. [PubMed: 16010006]

Maes M, Amit E, Danieli T, Lebendiker M, Loyter A, Friedler A. The disordered region of *Arabidopsis* VIP1 binds the *Agrobacterium* VirE2 protein outside its DNA-binding site. Protein Eng Des Sel. 2014; 27:439–446. [PubMed: 25212215]

Magori S, Citovsky V. *Agrobacterium* counteracts host-induced degradation of its F-box protein effector. Sci Signal. 2011; 4:ra69. [PubMed: 22009152]

Narasimhulu SB, Deng XB, Sarria R, Gelvin SB. Early transcription of *Agrobacterium* T-DNA genes in tobacco and maize. Plant Cell. 1996; 8:873–886. [PubMed: 8672885]

Notredame C, Higgins DG, Heringa J. T-Coffee: A novel method for fast and accurate multiple sequence alignment. J Mol Biol. 2000; 302:205–217. [PubMed: 10964570]

Pitzschke A, Djamei A, Teige M, Hirt H. VIP1 response elements mediate mitogen-activated protein kinase 3-induced stress gene expression. Proc Natl Acad Sci USA. 2009; 106:18414–18419. [PubMed: 19820165]

Saitou N, Nei M. The neighbor-joining method: a new method for reconstructing phylogenetic trees. Mol Biol Evol. 1987; 4:406–425. [PubMed: 3447015]

Sen P, Pazour GJ, Anderson D, Das A. Cooperative binding of *Agrobacterium tumefaciens* VirE2 protein to single-stranded DNA. J Bacteriol. 1989; 171:2573–2580. [PubMed: 2708313]

Shi Y, Lee LY, Gelvin SB. Is VIP1 important for *Agrobacterium*-mediated transformation? Plant J. 2014; 79:848–860. [PubMed: 24953893]

Stachel SE, An G, Flores C, Nester EW. A Tn3 *lacZ* transposon for the random generation of beta-galactosidase gene fusions: application to the analysis of gene expression in *Agrobacterium*. EMBO J. 1985; 4:891–898. [PubMed: 2990912]

Stachel SE, Nester EW. The genetic and transcriptional organization of the *vir* region of the A6 Ti plasmid of *Agrobacterium*. EMBO J. 1986; 5:1445–1454. [PubMed: 3017694]

Sutton A, Heller RC, Landry J, Choy JS, Sirko A, Sternglanz R. A novel form of transcriptional silencing by Sum1-1 requires Hst1 and the origin recognition complex. Mol Cell Biol. 2001; 21:3514–3522. [PubMed: 11313477]

Tamura K, Stecher G, Peterson D, Filipski A, Kumar S. MEGA6: Molecular Evolutionary Genetics Analysis version 6.0. Mol Biol Evol. 2013; 30:2725–2729. [PubMed: 24132122]

Tsugama D, Liu S, Takano T. A bZIP protein, VIP1, is a regulator of osmosensory signaling in *Arabidopsis*. Plant Physiol. 2012; 159:144–155. [PubMed: 22452852]

Tsugama D, Liu S, Takano T. Analysis of functions of VIP1 and its close homologs in osmosensory responses of *Arabidopsis thaliana*. PLOS ONE. 2014; 9:e103930. [PubMed: 25093810]

Tsugama D, Liu S, Takano T. The bZIP protein VIP1 is involved in touch responses in *Arabidopsis* roots. Plant Physiol. 2016; 171:1355–1365. [PubMed: 27208231]

Tzfira T, Tian GW, Lacroix B, Vyas S, Li J, Leitner-Dagan Y, et al. pSAT vectors: a modular series of plasmids for fluorescent protein tagging and expression of multiple genes in plants. Plant Mol Biol. 2005; 57:503–516. [PubMed: 15821977]

Tzfira T, Vaidya M, Citovsky V. VIP1, an *Arabidopsis* protein that interacts with *Agrobacterium* VirE2, is involved in VirE2 nuclear import and *Agrobacterium* infectivity. EMBO J. 2001; 20:3596–3607. [PubMed: 11432846]

Tzfira T, Vaidya M, Citovsky V. Increasing plant susceptibility to *Agrobacterium* infection by overexpression of the *Arabidopsis VIP1* gene. Proc Natl Acad Sci USA. 2002; 99:10435–10440. [PubMed: 12124400]

Tzfira T, Vaidya M, Citovsky V. Involvement of targeted proteolysis in plant genetic transformation by *Agrobacterium*. Nature. 2004; 431:87–92. [PubMed: 15343337]

Van Leene J, Blomme J, Kulkarni SR, Cannoot B, De Winne N, Eeckhout D, et al. Functional characterization of the Arabidopsis transcription factor bZIP29 reveals its role in leaf and root development. Journal of experimental botany. 2016; 67:5825–5840. [PubMed: 27660483]

Ward E, Barnes W. VirD2 protein of *Agrobacterium tumefaciens* very tightly linked to the 5′ end of T-strand DNA. Science. 1988; 242:927–930.

Wolf S, Deom CM, Beachy RN, Lucas WJ. Movement protein of tobacco mosaic virus modifies plasmodesmatal size exclusion limit. Science. 1989; 246:377–379. [PubMed: 16552920]

Young C, Nester EW. Association of the VirD2 protein with the 5′ end of T-strands in *Agrobacterium tumefaciens*. J Bacteriol. 1988; 170:3367–3374. [PubMed: 3403506]

Zaltsman A, Krichevsky A, Loyter A, Citovsky V. *Agrobacterium* induces expression of a plant host F-box protein required for tumorigenicity. Cell Host Microbe. 2010; 7:197–209. [PubMed: 20227663]

Zaltsman A, Lacroix B, Gafni Y, Citovsky V. Disassembly of synthetic *Agrobacterium* T-DNA-protein complexes via the host SCF^{VBF} ubiquitin-ligase complex pathway. Proc Natl Acad Sci USA. 2013; 110:169–174. [PubMed: 23248273]

Zuckerkandl, E., Pauling, L. Evolutionary divergence and convergence in proteins. In: Bryson, V., Vogel, HJ., editors. Evolving Genes and Proteins. Academic Press; New York: 1965. p. 97-166.

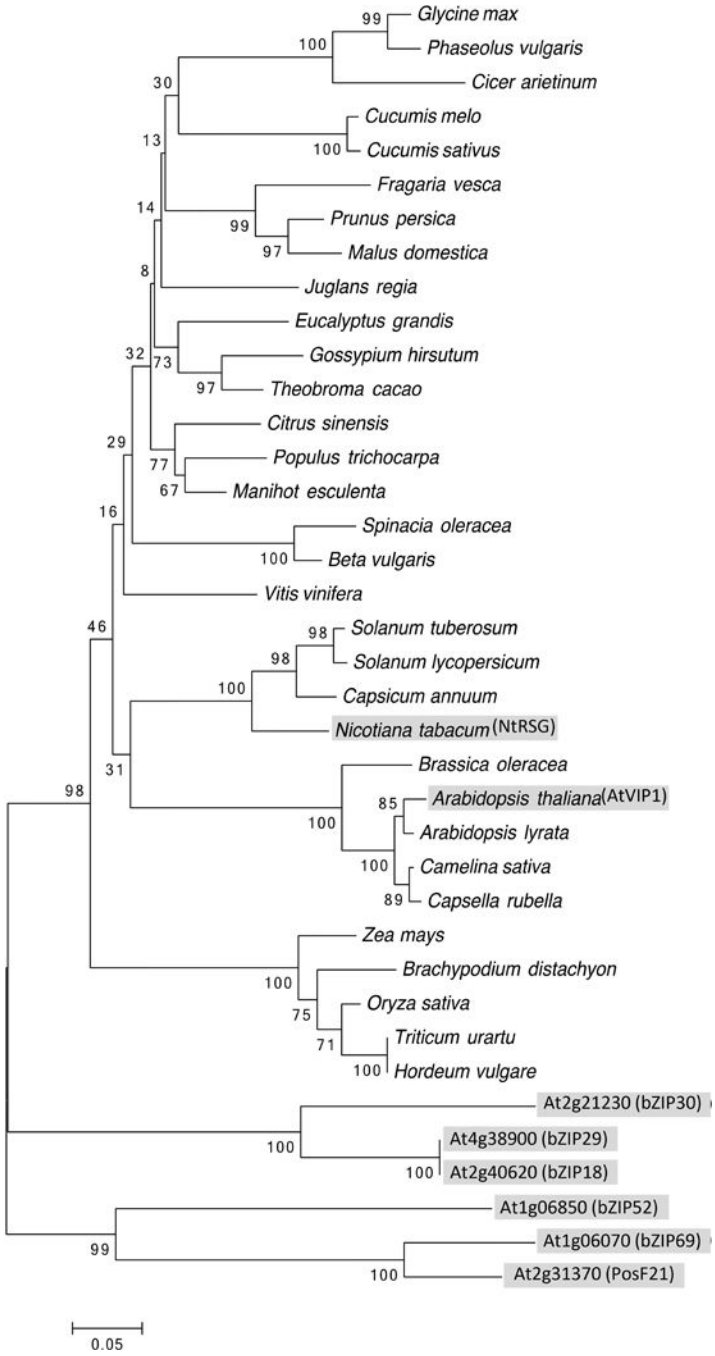

Fig. 1.

Phylogenetic tree of AtVIP1, its orthologs from representative plant species, and *Arabidopsis* homologs from the same subgroup. AtVIP1, its 6 closest *A. thaliana* homologs, and *N. tabacum* ortholog are highlighted by shaded boxes. The evolutionary history was inferred using the Neighbor-Joining method (Saitou & Nei, 1987). The optimal tree with the sum of branch length = 3.60596289 is shown. The percentage of replicate trees in which the associated taxa clustered together in the bootstrap test (1000 replicates) are shown next to the branches (Felsenstein, 1985). The tree is drawn to scale, with branch lengths in the same

units as those of the evolutionary distances used to infer the phylogenetic tree. The evolutionary distances were computed using the Poisson correction method (Zuckerkandl & Pauling, 1965) and are in the units of the number of amino acid substitutions per site. The analysis involved 38 amino acid sequences. All positions containing gaps and missing data were eliminated. There were a total of 179 positions in the final dataset. Evolutionary analyses were conducted using the Molecular Evolutionary Genetics Analysis tool (MEGA, version 6.0.5 for Mac OS) (http://www.megasoftware.net) (Tamura et al., 2013), which also generated this description of the analysis. Scale bar, 0.05 amino acid substitutions per site.

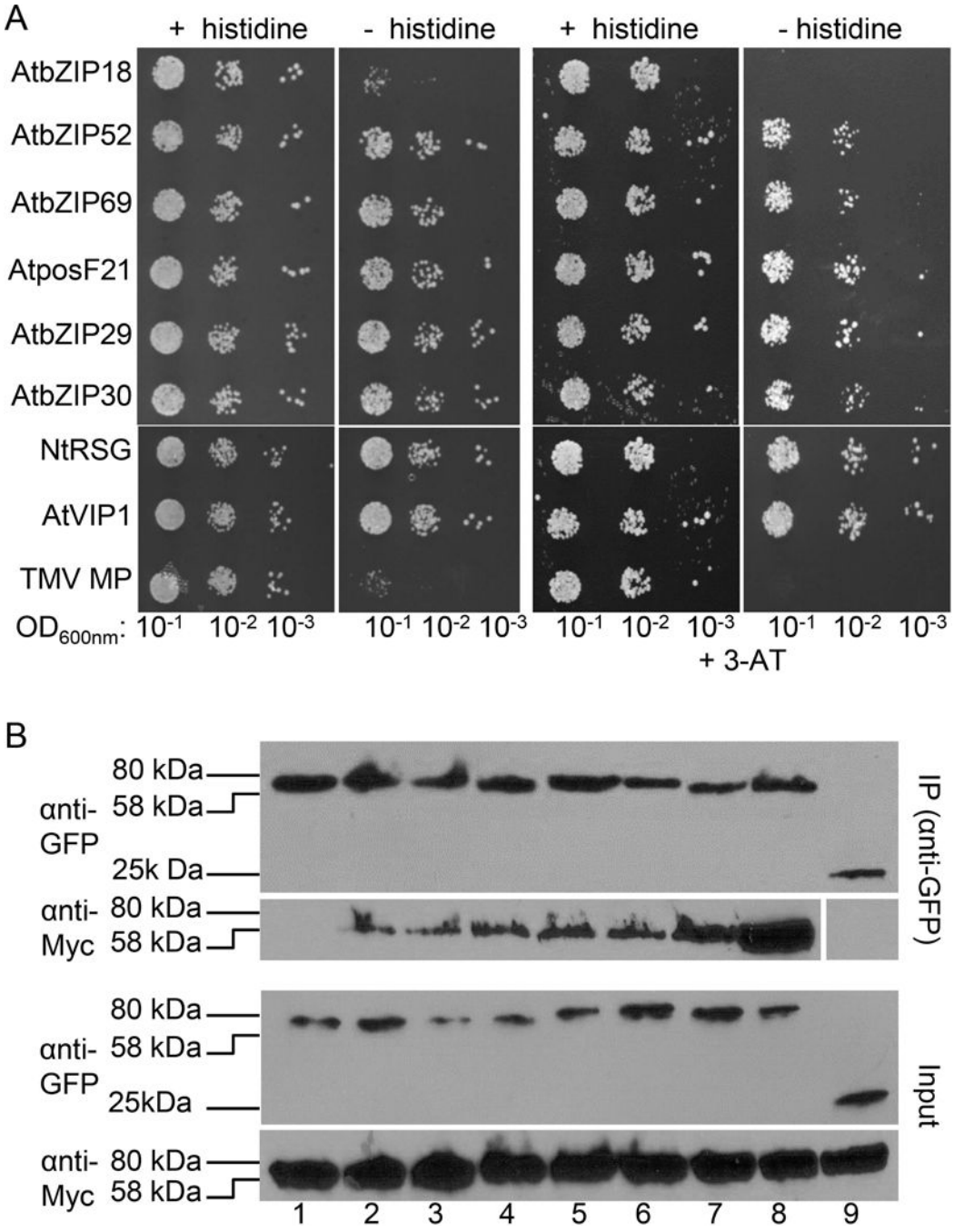

Fig. 2.

Interaction of *A. tumefaciens* C58 VirE2 with AtVIP1 and its homologs. (A) Yeast-two-hybrid interaction assay. LexA-C58 VirE2 was coexpressed with Gal4-AD fused to the indicated tested proteins. The indicated dilutions of cell cultures were plated and grown on non-selective (+ histidine) and selective media (− histidine) in the absence (left) or presence of 0.1 mM 3-AT (right). (B) Coimmunoprecipitation interaction assay. C58 VirE2-Myc was expressed with GFP-AtVIP1 and its GFP-tagged homologs for three days in agroinfiltrated *N. benthamiana* leaves, immunoprecipitated (IP) with anti-GFP antibody (top panel),

followed by western blot analysis with anti-GFP or anti-Myc antibody. To visualize the total amounts of the tested proteins (Input), they were analyzed by western blotting with anti-GFP or anti-Myc antibody without immunoprecipitation. Lane 1, AtbZIP18; lane 2, AtbZIP52; lane 3, AtbZIP69; lane 4, AtposF21; lane 5, AtbZIP29; lane 6, AtbZIP30; lane 7, NtRSG; lane 8, AtVIP1; lane 9, free GFP. Two independent experiments were performed for each assay with similar results.

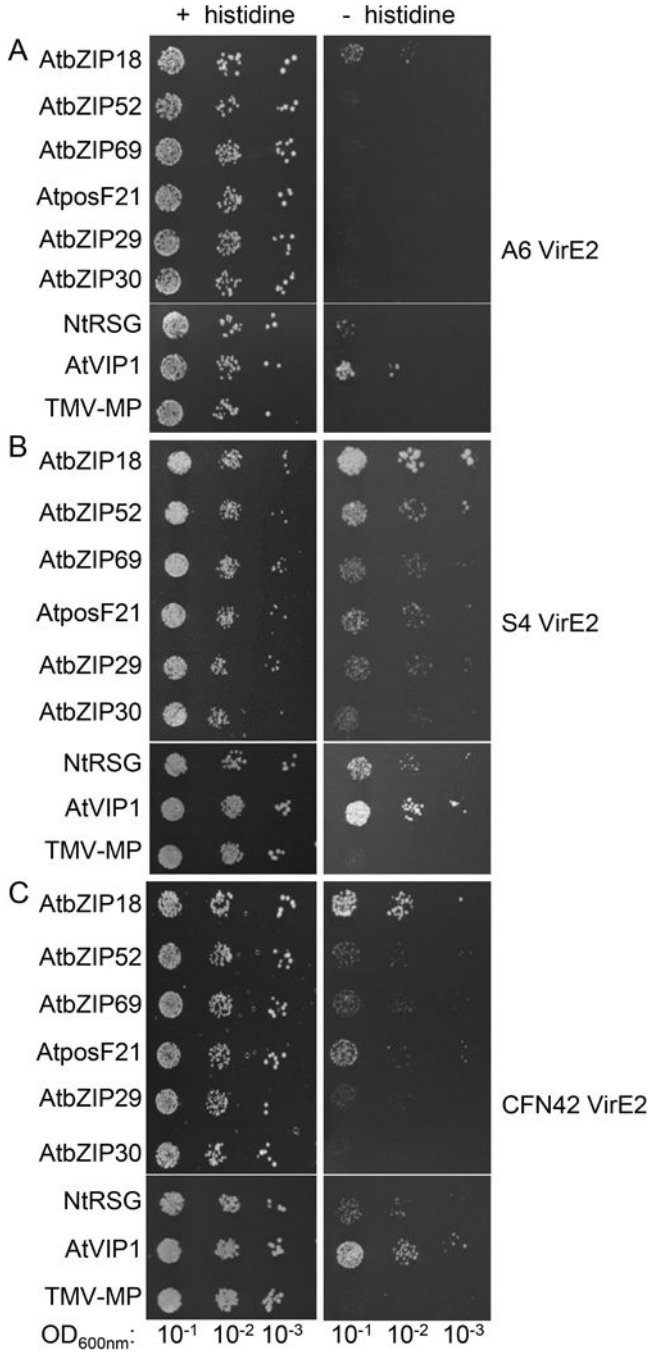

Fig. 3.

Interaction of VirE2 proteins from different *A. tumefaciens* and *R. etli* strains with AtVIP1 and its homologs. VirE2 proteins were fused to LexA and AtVIP1 and its homologs were fused to Gal4-AD. (A) *A. tumefaciens* A6 VirE2. Cells were grown presence of 0.1 mM 3-AT. (B) *A. vitis* S4 VirE2. Cells were grown presence of 1.0 mM 3-AT. (C) *R. etli* CFN42 VirE2. Cells were grown presence of 5.0 mM 3-AT. The indicated dilutions of cell cultures were plated and grown on non-selective (+ histidine) and selective media (- histidine). Two independent experiments were performed for each assay with similar results.

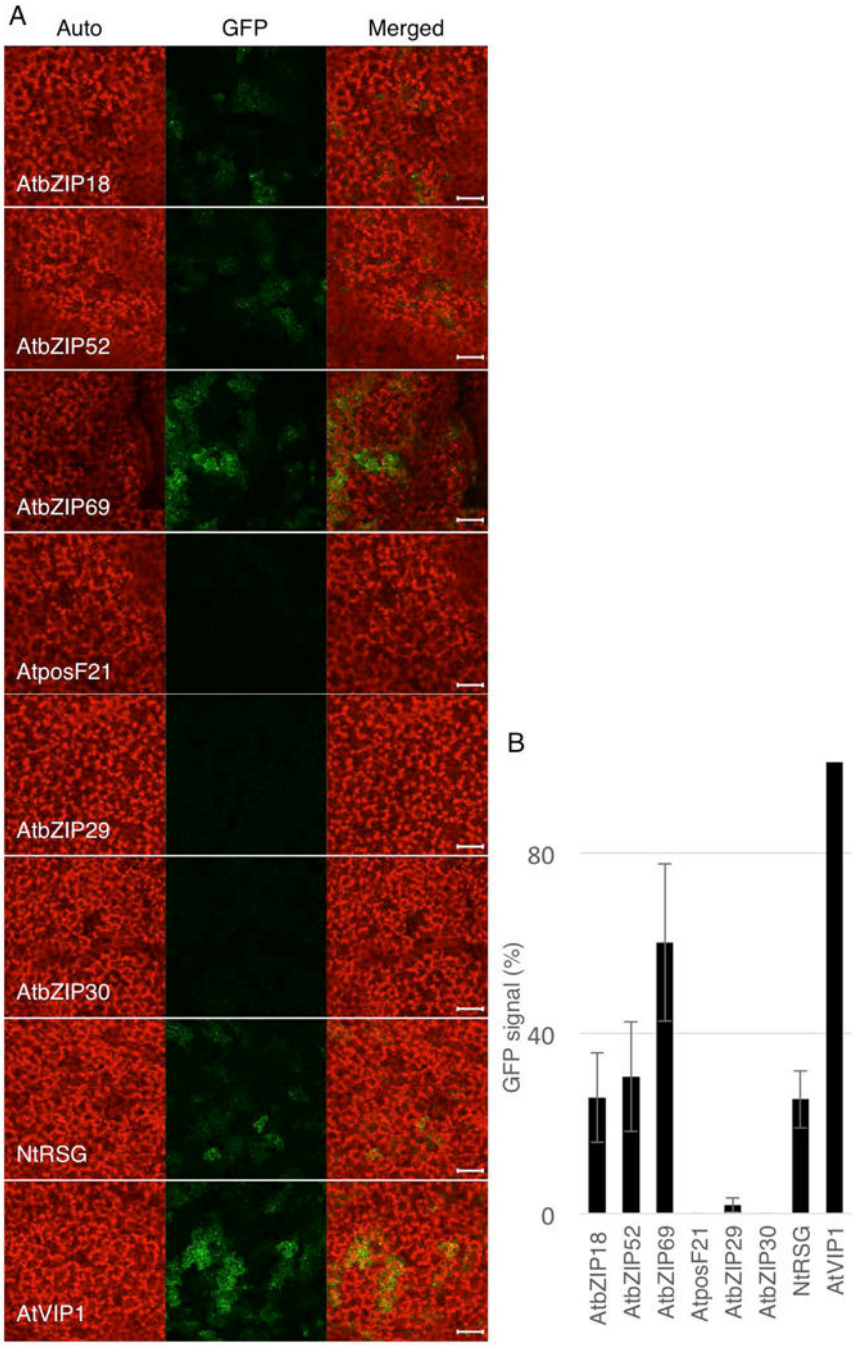

Fig. 4.

Induction of *VRE*-controlled GFP expression by AtVIP1 and its homologs. (A) Confocal microscopy analysis of GFP expression in *N. benthamiana* leaves three days after co-infiltration with two *Agrobacterium* strains carrying the *VRE1-35Smin-GFP* reporter construct and a construct expressing AtVIP1 or its indicated homologs. GFP signal is in green; plastid autofluorescence is in red. Images are single confocal sections, and they are representative of images obtained in three infiltrations performed on three different leaves, with two images recorded per infiltration. Scale bars = 100 μm. (B) Quantification of the

VRE1-GFP reporter expression shown in (A). GFP signal was quantified using the LSM Pascal software (Zeiss) by measuring the total GFP fluorescence in one field inside the infiltration area with a low magnification objective (10×); all images used for fluorescence measurement were taken with the same settings. Basal signal measured in area infiltrated with *VRE1-GFP* alone was subtracted from the values measured for each experimental condition, and the signal obtained with AtVIP1 was set as 100%. Error bars represent SEM of N=3 independent biological replicates (leaves).

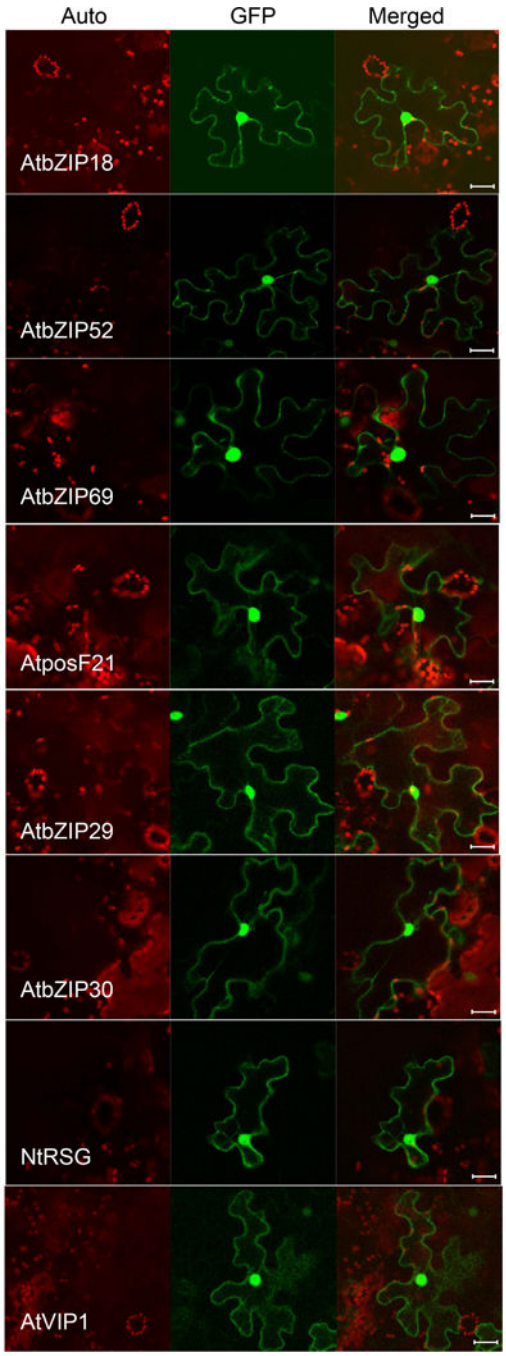

Fig. 5.

AtVIP1and its homologs localize to the cell nucleus and cytoplasm. The indicated proteins tagged with GFP were transiently expressed in agroinfiltrated leaf epidermis of *N. benthamiana*, and analyzed by confocal microscopy three days post-infiltration. GFP signal is in green, plastid autofluorescence is in red. Images are single confocal sections, representative of images obtained in two independent experiments performed for each protein; for each experiment, three infiltrations were performed on three different leaves, with two images recorded per infiltration. Scale bars= 20 μM.

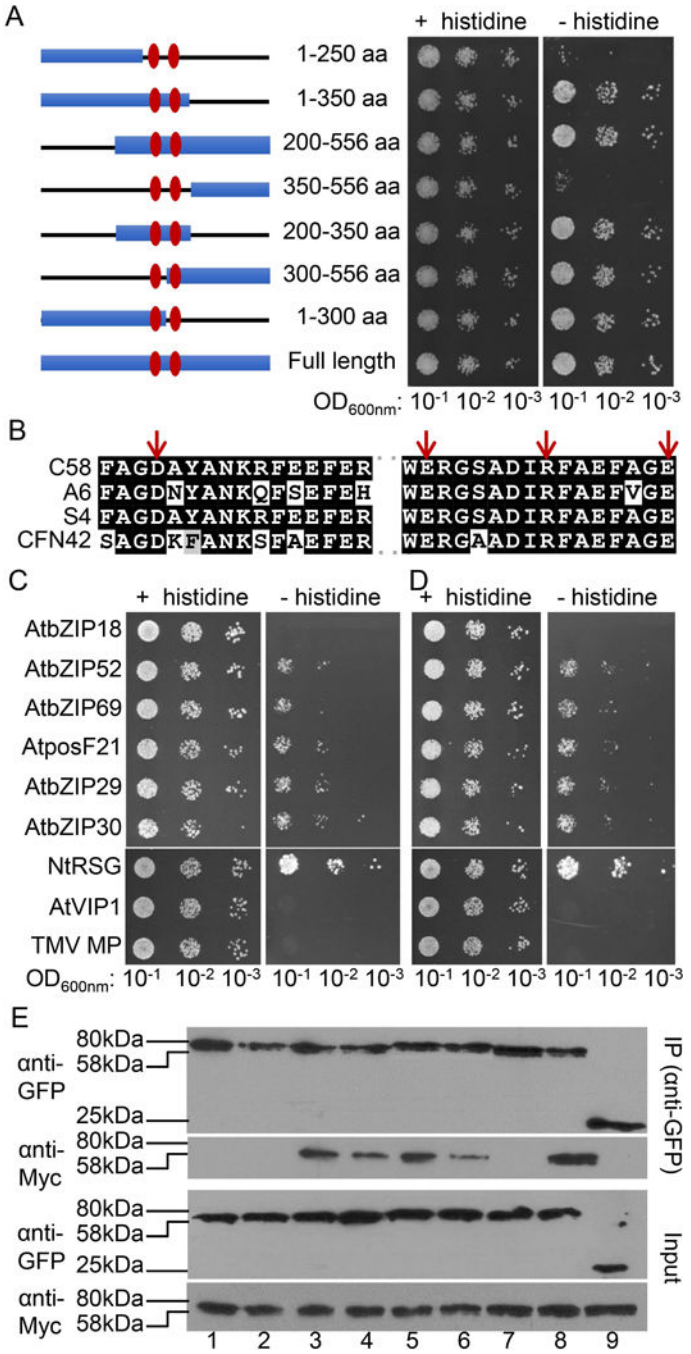

Fig. 6.

Interaction of C58 VirE2 mutants with AtVIP1 and its homologs. (A) A schematic summary of C58 VirE2 deletion mutants (left) and yeast-two-hybrid assay for interaction between the indicated C58 VirE2 mutants fused to LexA and AtVIP1 fused to Gal4-AD (right). Numbers represent the positions of amino acid residues present in each mutant, and the two central domains are indicated with vertical ovals. The indicated dilutions of cell cultures were plated and grown on non-selective (+ histidine) and selective media (- histidine) in the presence of 0.1 mM 3-AT. (B) Amino acid sequence alignment of the two central domains in C58 VirE2,

A6 VirE2, S4 VirE2, and CFN42 VirE2. The residues mutated in the C58 VirE2 4M mutant, i.e., D281, E324, R331, and E338, are indicated with arrows. (C) Yeast-two-hybrid assay for C58 VirE2 4M interactions with AtVIP1 and its homologs. (D) Yeast-two-hybrid assay for C58 VirE2 350–556 interactions with AtVIP1 and its homologs. LexA-C58 VirE2 4M or LexA-C58 VirE2 350–556 was coexpressed with Gal4-AD fused to the indicated tested proteins. The indicated dilutions of cell cultures were plated and grown on non-selective (+ histidine) and selective media (- histidine) in the presence of 0.1 mM 3-AT. (E) Coimmunoprecipitation assay for C58 VirE2 4M interactions with AtVIP1 and its homologs. The experiment was performed using C58 VirE2 4M-Myc exactly as described in Fig. 2B for a similar assay with C58 VirE2-Myc. Top panel, proteins immunoprecipitated (IP) with anti-GFP antibody and analyzed by western blotting with anti-GFP antibody or anti-Myc antibody. Bottom panel, total amounts of the tested proteins (Input) analyzed by western blotting with anti-GFP or anti-Myc antibody without immunoprecipitation. Lane 1, AtbZIP18; lane 2, AtbZIP52; lane 3, AtbZIP69; lane 4, AtposF21; lane 5, AtbZIP29; lane 6, AtbZIP30; lane 7, NtRSG; lane 8, AtVIP1; lane 9, free GFP. Two independent experiments were performed for each assay with similar results.

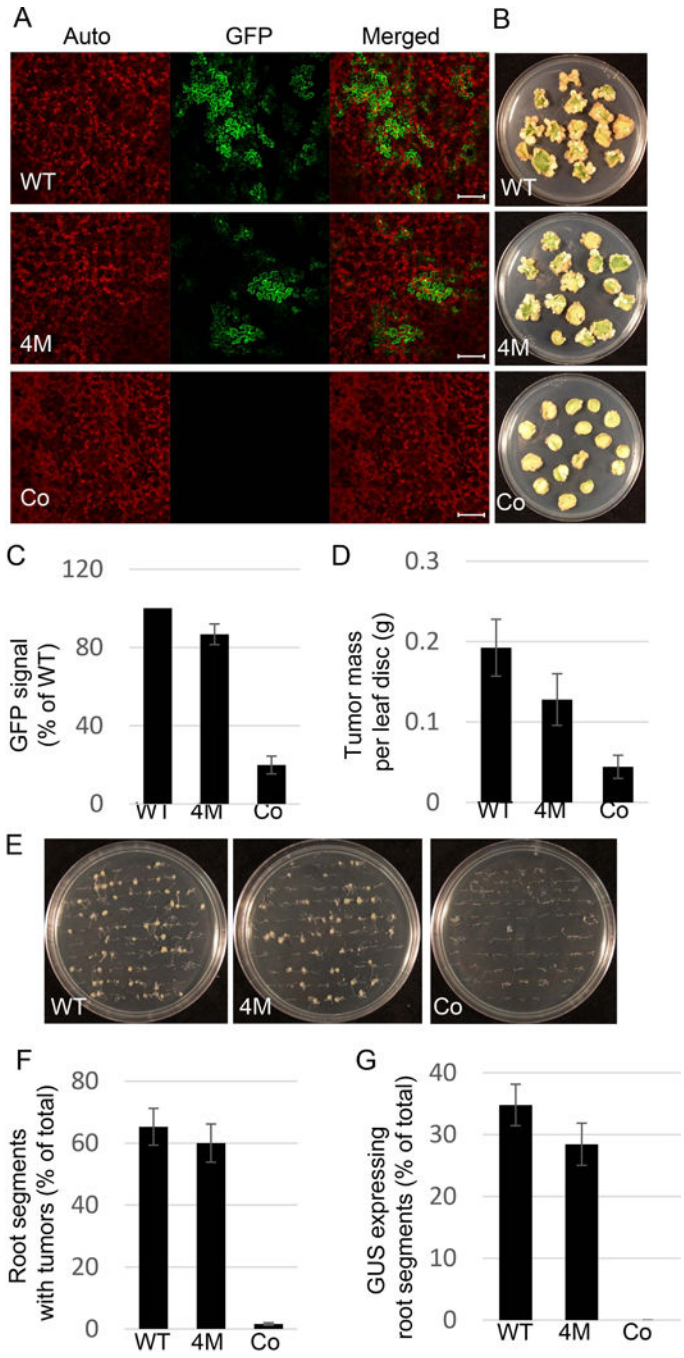

Fig. 7.

The effect of C58 VirE2 4M on transient and stable transformation capacity of *Agrobacterium*. (A) Transient transformation of *N. benthamiana* leaves. Plant tissues were coinfiltrated with two cultures of the *Agrobacterium* strain mx358 that lacks its endogenous *vir*E2 gene: one harboring a plasmid that expresses either wild-type C58 VirE2 (pEpA6-C58*vir*E2) or C58 VirE2 4M (pEpA6-C58*vir*E2–4M) in the bacterium, or carries an empty plasmid (pEpA6), and the other harboring a binary plasmid that expresses the GFP reporter. Three days post-infiltration, GFP expression in the inoculated tissues was analyzed by

confocal microscopy. GFP signal is in green, plastid autofluorescence is in red. Images are single confocal sections, representative of images obtained in two independent experiments performed for each protein; for each experiment, three infiltrations were performed on three different leaves, with two images recorded per infiltration. Scale bars= 100 μM. (B) Stable transformation of *N. tabacum* leaves. Leaf discs were inoculated with the *Agrobacterium* strain mx358 with a plasmid that expresses either wild-type C58 VirE2 (pEpA6-C58*vir*E2) or C58 VirE2 4M (pEpA6-C58*vir*E2-4M), or carries an empty plasmid (pEpA6), and the tumors were photographed three weeks after inoculation. Three plates, each containing 15 leaf discs, were used for each condition. (C) Quantification of GFP expression shown in (A). GFP signal was quantified as described in Fig. 4. Signal obtained with wild-type C58 VirE2 was set as 100%. Error bars represent SEM of N=3 independent biological replicates (leaves). (D) Quantification of tumor formation shown in (B). Tumors were scored by their mass. Error bars represent SEM of N=3 independent biological replicates (plates). (E) Stable transformation of *A. thaliana* roots. Root segments were inoculated with the *Agrobacterium* strain mx358 with a plasmid that expresses either wild-type C58 VirE2 (pEpA6-C58*vir*E2) or C58 VirE2 4M (pEpA6-C58*vir*E2-4M), or carries an empty plasmid (pEpA6), and the tumors were photographed three weeks after inoculation. Three plates, each containing 50 root segments, were used for each condition. (F) Quantification of tumor formation shown in (E). Roots segments with tumors were counted and expressed as percent of the total inoculated roots. Error bars represent SEM of N=3 independent biological replicates (plates). (G) Transient transformation of *A. thaliana* roots. Root segments were inoculated with two cultures of the *Agrobacterium* strain mx358: one with a plasmid expressing wild-type C58 VirE2 (pEpA6-C58*vir*E2) or C58 VirE2 4M (pEpA6-C58*vir*E2-4M), or carries an empty plasmid (pEpA6), and the other harboring a binary plasmid expressing the GUS reporter. Three days post-inoculation, GUS activity in the inoculated tissues was analyzed by histochemical staining, and the number of stained roots counted and expressed as percent of the total inoculated roots. Three plates, each containing 50 root segments, were used for each condition. WT, wild-type C58 VirE2; 4M, C58 VirE2 4M; Co, empty vector.